

A Recursive Method for the Approximation of LTI Systems Using Subband Processing

Damián Marelli and Minyue Fu, *Fellow, IEEE*

Abstract—Using the subband technique, an LTI system can be implemented by the composition of an analysis filterbank, followed by a transfer matrix (subband model) and a synthesis filterbank. The advantage of this approach is that it offers a good tradeoff between latency and computational complexity. In this paper we propose an optimization method for approximating an LTI system using the subband technique. The proposed method includes optimal allocation of parameters from different FIR entries of the subband model, while keeping constant the total number of parameters, for a better utilization of the available coefficients. The optimization is done in a weighted least-squares sense considering either linear or logarithmic amplitude scale. Simulation results demonstrate the advantages of the proposed method when compared with classical implementation approaches using pole-zero transfer functions or segmented FFT algorithms.

Index Terms—Modeling, system analysis and design, subband signal processing.

I. INTRODUCTION

AN LTI system can be implemented in the time-domain using direct convolution. When the order of the impulse response ranges from several hundred to a few thousand taps, this approach is computationally inefficient and often prohibitive for real-time applications (e.g., in audio signal processing). A computationally efficient alternative implements the system in the frequency domain. However, this approach is equally unsuitable for real-time applications since it requires block processing of the “whole history of the involved signals, introducing large latency (i.e., implementation delay). Even when applying the so-called overlap-save and overlap-add (OS/A) methods [1], which permit efficient implementation of a finite impulse response (FIR) approximation of the LTI system, delays can be reduced only to a limited extent. To further reduce the delay, a low latency fast convolution algorithm was introduced in [2]. This algorithm splits the impulse response into a number of segments which are processed using OS/A methods, while the first segment can be optionally processed in the time domain to eliminate the latency. The latency reduction can be accommodated by varying the number of segments,

and is obtained at the expense of increasing the computational complexity. All the methods, collectively called segmented FFT methods, accommodate a tradeoff between computational complexity and latency [3]. These are attractive options for applications where some delay can be afforded, but reduced computational efficiency is a main side effect.

A different approach for modeling LTI systems uses pole-zero transfer functions [4]–[9]. The advantage of this approach is that it approximates an LTI system with a very large impulse responses without implementation latency. However, a large number of poles and zeros may be needed to achieve a small approximation error, hence, it is often less numerically efficient than segmented FFT methods [10], [11]. Also, the coefficients of a pole-zero model are sensitive to quantization errors [1, Ch. 7.6], which can cause robustness and stability problems, especially in implementations using fixed point arithmetic.

A recently proposed alternative approach implements the system in the subband (i.e., time-frequency) domain [12], [13]. Using this subband technique, a linear system is implemented by the composition of an analysis filterbank, followed by a transfer matrix (*subband model*) and a synthesis filterbank. This approach has also been used for system identification [14], adaptive filtering [15], [16], channel equalization [17], etc., with the advantage of having high numerical efficiency. The approximation of LTI systems using the subband technique was studied in [12] for the critical sampling subband scheme (where the downsampling factor equals the number of subbands). A step further in this direction was taken in [13], where a more general oversampling subband scheme (where the downsampling factor is smaller than or equal to the number of subbands) was used, and the subband model was optimally chosen in a least-squares (LS) sense.

In this paper we extend the result from [13] as follows: First, we propose an iterative algorithm to jointly optimize the subband model, the analysis and the synthesis filterbanks in a weighted least-squares (WLS) sense. The algorithm includes the adaptive allocation of parameters from different FIR entries of the (matrix) subband model, while keeping constant the total number of parameters, for a better utilization of the available coefficients. We then propose another iterative algorithm where a weighted logarithmic-least-squares (WLogLS) criterion is used for optimization. This criterion is motivated by the fact that the human auditory system perceives the amplitude of the frequency contents of a sound signal in a logarithmic scale [18], and therefore aims at audio signal processing applications.

In order to illustrate the applicability of the proposed method we introduce two examples. The first one considers a WLS criterion to approximate the inverse of a multipath communication channel. The second one considers a WLogLS approxima-

Manuscript received August 26, 2009; accepted September 11, 2009. First published October 20, 2009; current version published February 10, 2010. This work was partially developed at the Faculty of Mathematics, NuHAG, University of Vienna, with support from the EU Marie Curie fellowship MEIF-CT-2006-023728. The associate editor coordinating the review of this manuscript and approving it for publication was Prof. Antonia Papandreou-Suppappola.

The authors are with the School of Electrical Engineering and Computer Science, University of Newcastle, N.S.W. 2308 Australia (e-mail: damian.marelli@newcastle.edu.au; minyue.fu@newcastle.edu.au).

Color versions of one or more of the figures in this paper are available online at <http://ieeexplore.ieee.org>.

Digital Object Identifier 10.1109/TSP.2009.2034933

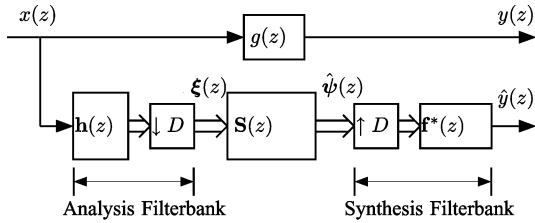


Fig. 1. System approximation using subband processing.

tion criterion for implementation of head-related transfer functions (HRTFs), which find applications in the so-called binaural virtual acoustics synthesis [19], [20]. Simulation results show that the subband method, designed using the proposed method, is more efficient than segmented FFT methods and pole-zero models, while keeping the latency and approximation error within prescribed tolerances.

The rest of the paper is organized as follows: In Section II we state the problem of approximating an LTI system using subbands. In Section III we use the polyphase representation to provide a mathematical setting for deriving, in Section IV the proposed optimization algorithm. In Section V we explain how to modify the proposed algorithm to carry out the optimization in a logarithmic amplitude scale. The application of the proposed method is illustrated in Section VI using numerical simulations, and concluding comments are given in Section VII. For the ease of readability, all proofs are contained in the Appendix.

Throughout the paper we will use the following notational convention: Scalars are denoted using normal (i.e., nonbold) lowercase letters (e.g., x); and vector and matrix using lowercase bold letters (e.g., \mathbf{x}) and uppercase bold letters (e.g., \mathbf{X}), respectively. The i th entry of a vector \mathbf{x} is denoted by $[\mathbf{x}]_i$ and the i, j th entry of a matrix \mathbf{X} is denoted by $[\mathbf{X}]_{i,j}$.

II. LTI SYSTEM IMPLEMENTATION USING SUBBAND PROCESSING

The subband technique for approximating a linear system is depicted in Fig. 1. The linear system $g(z)$ is approximated by splitting the input signal $x(z)$ into M subbands using an array of filters $\mathbf{h}(z) = [h_1(z), \dots, h_M(z)]^T$, followed by a downsampling operation of factor D (by keeping one out of D samples). In this way, the subband signal $\boldsymbol{\xi}(z) = [\xi_1(z), \dots, \xi_M(z)]^T$ is generated, which is called the subband representation of the (fullband) signal $x(z)$. The subband model is an $M \times M$ transfer matrix $\mathbf{S}(z)$ whose output is denoted by $\hat{\boldsymbol{\psi}}(z) = [\hat{\psi}_1(z), \dots, \hat{\psi}_M(z)]^T$. The output signal $\hat{y}(z)$ is generated by upsampling $\hat{\boldsymbol{\psi}}(z)$ by a factor of D (by inserting $D - 1$ zeros between every two samples), then filtering each component using an array of filters $\mathbf{f}^*(z) = [f_1^*(z), \dots, f_M^*(z)]$, and finally adding together all the resulting signals.

We will assume that the filters in the arrays $\mathbf{h}(z)$ and $\mathbf{f}(z)$ are FIR, having tap sizes l_h and l_f , respectively. Also, to simplify the notation, and without loss of generality, we will assume that they are causal. The entries of the subband model $\mathbf{S}(z)$ are FIR filters whose supports are defined by two matrices $\mathbf{P}, \mathbf{Q} \in \mathbb{Z}^{M \times M}$ as follows: for each $i, j = 1, \dots, M$, $[\mathbf{S}(z)]_{i,j} = 0$ for all $t \notin \{[\mathbf{P}]_{i,j}, \dots, [\mathbf{Q}]_{i,j}\}$. The total number of parameters of

TABLE I
COMPUTATIONAL COST (CC) AND LATENCY OF THE SUBBAND METHOD

| CC [real mult./sample] | $\frac{2l_s + l_h + l_f}{D} + \frac{4M}{D} \log_2 M$ |
|------------------------|--|
| Latency [samples] | $n_s D + l_f - 1$ |

the subband model $\mathbf{S}(z)$ is denoted by $l_s = \sum_{i,j=1}^M ([\mathbf{Q}]_{i,j} - [\mathbf{P}]_{i,j} + 1)$, and its latency by $n_s = -\min_{i,j} [\mathbf{P}]_{i,j}$. We assume that the filterbanks are of Gabor type, i.e., there exists a prototype filter $h_m(z)$ such that $h_m(z) = h(e^{j2\pi m-1/M} z)$ for all $m = 1, \dots, M$ and all $t \in \mathbb{Z}$, and a similar condition holds for $f_m(z), m = 1, \dots, M$. Gabor filterbanks offer less flexibility than generic filterbanks, but they can be implemented in a numerically efficient way using FFT [21], and they turn out to outperform generic filterbanks in the tradeoff between computational complexity and approximation error.

Using the algorithm in [21], and assuming that M is a power of two, so that an M -point FFT can be implemented with $2M \log_2 M$ (real) multiplications using the Radix-2 algorithm [11, Ch. 6.1], the implementation of both the analysis and the synthesis filterbanks require $(l_h + l_f + 4M \log_2 M)/D$ real multiplications per (fullband) sample. Also, assuming that the input signal $x(t)$ is real valued, only half of the subband model $\mathbf{S}(z)$ entries need to be computed. Using these remarks, we show in Table I the computational cost required to implement an LTI system using the subband method, together with its associated latency.

As pointed out in Remark 1, the system $x \mapsto \hat{y}$ induced by the subband technique from input to output is D -cyclostationary (i.e., there exists a set of D impulse responses $\hat{g}_d(t)$, $d = 0, \dots, D-1$ such that $\hat{y}(t) = \sum_{\tau \in \mathbb{Z}} \hat{g}_{t \bmod D}(\tau) x(t - \tau)$). In view of this, the design problem becomes finding, for given values of l_h, l_f, l_s, M and D , the prototype filters $h(z)$ and $f(z)$, and the subband model $\mathbf{S}(z)$ (including the matrices \mathbf{P} and \mathbf{Q} defining its support), that solve the following WLS minimization problem:

$$[h, f, \mathbf{S}] = \arg \min_{h, f, \mathbf{S}, \mathbf{P}, \mathbf{Q}} \frac{1}{D} \times \sum_{d=0}^{D-1} \frac{1}{2\pi} \int_{-\pi}^{\pi} w(e^{j\omega}) |g(e^{j\omega}) - \hat{g}_d(e^{j\omega})|^2 d\omega \quad (1)$$

where $w(z)$ is a user-supplied spectral weighting function which needs to be real and positive on the unit circle.

III. A RESTATEMENT OF (1) USING POLYPHASE REPRESENTATION

The aim of this section is to express (1) in a mathematically more tractable way. To this end, we use the so-called polyphase representation [22].

A. Polyphase Representation

The polyphase representation of a scalar signal $x(t)$ is the D -dimensional vector signal $\mathbf{x}(t)$ defined by

$$[\mathbf{x}(t)]_d = x(tD + 1 - d), \text{ for all } d = 1, \dots, D.$$

Also, the polyphase representation of a D -cyclostationary linear system with impulse responses $g_d(t)$, $d = 0, \dots, D - 1$, is the $D \times D$ impulse response matrix $\mathbf{G}(t)$ defined by

$$[\mathbf{G}(t)]_{d,e} = g_d(tD + e - d), \text{ for all } d, e = 1, \dots, D. \quad (2)$$

The polyphase representation enjoys the following properties:

(P1) The polyphase representations $\mathbf{x}(z)$ and $\mathbf{y}(z)$ of the input $x(z)$ and output $y(z)$ of a D -cyclostationary system with polyphase representation $\mathbf{G}(z)$ are related by $\mathbf{y}(z) = \mathbf{G}(z)\mathbf{x}(z)$.

(P2) The polyphase representation $\mathbf{E}(z)$ of the system formed by the concatenation of D -cyclostationary systems with polyphase representations $\mathbf{F}(z)$ and $\mathbf{G}(z)$ is given by $\mathbf{E}(z) = \mathbf{G}(z)\mathbf{F}(z)$.

The polyphase representation of an analysis filterbank with filters $h_m(z)$, $m = 1, \dots, M$, and downsampling factor D is the $D \times D$ transfer matrix $\mathbf{H}(z)$ defined by

$$\begin{aligned} [\mathbf{H}(t)]_{m,d} &= h_m(tD + d - 1) \\ \text{for all } m &= 1, \dots, M \text{ and } d = 1, \dots, D. \end{aligned} \quad (3)$$

Also, the polyphase representation of a synthesis filterbank with filters $f_m(z)$, $m = 1, \dots, M$, and upsampling factor D is given by $\mathbf{F}^*(z)$, where $\mathbf{F}(z)$ is defined in a way similar to (3), and $\mathbf{F}^*(z)$ denotes the transpose conjugate of $\mathbf{F}(z)$.

If $\mathbf{h}(z)$ is of Gabor type, and the prototype filter $h(z)$ is causal with tap size l_h , then its polyphase representation is given by [21]

$$\mathbf{H}(z) = \mathcal{W}_M \mathbf{L}_2 \Lambda_h \mathbf{L}_1(z) \quad (4)$$

where $\mathcal{W}_M \in \mathbb{C}^{M \times M}$ is the DFT matrix, i.e., $[\mathcal{W}_M]_{k,l} = e^{-j2\pi/Mkl}$ and

$$\begin{aligned} \mathbf{L}_1^T(z) &= [\mathbf{I}_D, \dots, z^{-a+1} \mathbf{I}_D]_{:,1:l_h} \\ \mathbf{L}_2 &= \underbrace{[\mathbf{I}_M, \mathbf{I}_M, \dots, \mathbf{I}_M]_{:,1:l_h}}_{b \text{ times}} \\ \Lambda_h &= \text{diag}\{h(0), \dots, h(l_h - 1)\} \end{aligned}$$

with $a = \lceil l_h/D \rceil$, $b = \lceil l_h/M \rceil$ ($\lceil x \rceil$ denotes the nearest integers greater than or equal to x), $[\mathbf{A}]_{:,1:l_h}$ denoting the matrix formed with the first l_h columns of \mathbf{A} , and $\text{diag}\{x_1, \dots, x_l\}$ denoting the diagonal matrix with elements $\{x_1, \dots, x_l\}$ in its main diagonal.

B. Restatement of the Approximation Criterion (1)

Using the polyphase representation, the scheme in Fig. 1 can be represented by the LTI system shown in Fig. 2, i.e.

$$\mathbf{y}(z) = \mathbf{G}(z)\mathbf{x}(z) \quad (5)$$

$$\hat{\mathbf{y}}(z) = \mathbf{F}^*(z)\mathbf{S}(z)\mathbf{H}(z)\mathbf{x}(z). \quad (6)$$

Then, as shown in the Appendix, (1) is equivalent to

$$[h, f, \mathbf{S}] = \arg \min_{h, f, \mathbf{S}, \mathbf{P}, \mathbf{Q}} \|\mathbf{G} - \mathbf{F}^* \mathbf{S} \mathbf{H}\|_{\mathbf{W}} \quad (7)$$

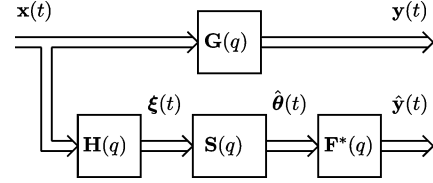


Fig. 2. Polyphase representation of the subband system approximation scheme.

where the norm $\|\cdot\|_{\mathbf{W}}$ is defined by

$$\|\mathbf{X}\|_{\mathbf{W}}^2 = \frac{1}{2\pi D} \int_{-\pi}^{\pi} \text{Tr} \{ \mathbf{X}(e^{j\omega}) \mathbf{W}(e^{j\omega}) \mathbf{X}^*(e^{j\omega}) \} d\omega \quad (8)$$

with $\mathbf{W}(z)$ being the polyphase representation of $w(z)$ and $\text{Tr}\{\mathbf{A}\} = \sum_i [\mathbf{A}]_{i,i}$ denoting the trace operator.

Remark 1: Equation (6) states that the input-output relation induced by the subband technique is given by the $D \times D$ polyphase matrix $\mathbf{F}^*(z)\mathbf{S}(z)\mathbf{H}(z)$. Also, (2) states that all $D \times D$ polyphase matrices correspond to the polyphase representation of a D -cyclostationary system. Hence, it follows that, for any choice of filterbanks $\mathbf{h}(z)$ and $\mathbf{f}(z)$ and any subband model $\mathbf{S}(z)$, the system $x \mapsto \hat{y}$ induced by the subband technique is D -cyclostationary.

IV. OPTIMIZATION ALGORITHM

In this section, we propose an optimization algorithm to solve (7). Suppose \mathbf{P} and \mathbf{Q} are given, then (7) becomes a nonlinear LS optimization problem, which could in principle be solved using any Newton-like search algorithm as described in [23]. However, notice that if we only consider the optimization with respect to either \mathbf{S} , h or f , the problem becomes a linear LS (LLS) one. Hence, it can be solved using the simpler alternating LS (ALS) algorithm, i.e., by cyclically optimizing $\mathbf{S}(z)$, $h(z)$ and $f(z)$. On the other hand, if $h(z)$ and $f(z)$ are given, then \mathbf{P} and \mathbf{Q} can be obtained using the orthogonal matching pursuit (OMP) algorithm, as described in Section IV-D below. Then, we propose the following algorithm:

- 1) **Initialization:** Obtain initial values of $h(z)$ and $f(z)$ (to be described in Section IV-E).
- 2) **Main iterations:** Cyclically iterate the following two steps, until the approximation error stops decreasing.
 - a) **OMP algorithm:** Obtain \mathbf{P} and \mathbf{Q} using the OMP algorithm (to be described in Section IV-D).
 - b) **ALS algorithm:** Cyclically optimize $\mathbf{S}(z)$, $h(z)$ and $f(z)$ using the LLS method (to be described in Sections IV-A–C, respectively) until the error reduction falls within a given tolerance.

In Sections IV-A–E below, we describe each step separately. The proofs are in the Appendix.

A. Optimization of $h(z)$

The solution of (7), for fixed choices of $f(z)$, $\mathbf{S}(z)$, \mathbf{P} and \mathbf{Q} , is given by

$$h(z) = \Omega_{l_h}(z) \underline{\mathbf{M}}_{l_h}^\dagger \underline{\mathbf{v}}_{l_h} \quad (9)$$

where $\Omega_h(z) = [1, z^{-1}, \dots, z^{-l_h+1}]$ and

$$\begin{aligned}\mathbf{v}_h &= \frac{1}{2\pi} \int_{-\pi}^{\pi} \text{diag}^{-1} \{ \mathbf{V}_h(e^{j\omega}) \} d\omega \\ \underline{\mathbf{M}}_h &= \frac{1}{2\pi} \int_{-\pi}^{\pi} \mathbf{M}_h(e^{j\omega}) d\omega.\end{aligned}$$

The expression, $\text{diag}^{-1}\{\mathbf{X}\}$ denotes a column vector containing the diagonal entries of the matrix \mathbf{X} and

$$\begin{aligned}\mathbf{V}_h(z) &= \mathbf{L}_2^* \mathcal{W}_M^* \mathbf{S}^*(z) \mathbf{F}(z) \mathbf{G}(z) \mathbf{W}(z) \mathbf{L}_1^*(z) \\ \mathbf{M}_h(z) &= \mathbf{M}_{h,1}(z) \odot \mathbf{M}_{h,2}^T(z)\end{aligned}$$

with

$$\begin{aligned}\mathbf{M}_{h,1}(z) &= \mathbf{L}_2^* \mathcal{W}_M^* \mathbf{S}^*(z) \mathbf{F}(z) \mathbf{F}^*(z) \mathbf{S}(z) \mathcal{W}_M \mathbf{L}_2 \\ \mathbf{M}_{h,2}(z) &= \mathbf{L}_1(z) \mathbf{W}(z) \mathbf{L}_1^*(z)\end{aligned}$$

and $\mathbf{X} \odot \mathbf{Y}$ denoting point-wise matrix product, i.e., $[\mathbf{X}(z) \odot \mathbf{Y}(z)]_{i,j} = [\mathbf{X}(z)]_{i,j} [\mathbf{Y}(z)]_{i,j}$ for all i and j .

B. Optimization of $f(z)$

The solution of (7), for fix choices of $h(z)$, $\mathbf{S}(z)$, \mathbf{P} , and \mathbf{Q} , is given by

$$f(z) = \Omega_f(z) \underline{\mathbf{M}}_f^\dagger \mathbf{v}_f \quad (10)$$

where $\Omega_f(z) = [1, z^{-1}, \dots, z^{-l_f+1}]$ and

$$\begin{aligned}\mathbf{v}_f &= \frac{1}{2\pi} \int_{-\pi}^{\pi} \text{diag}^{-1} \{ \mathbf{V}_f(e^{j\omega}) \} d\omega \\ \underline{\mathbf{M}}_f &= \frac{1}{2\pi} \int_{-\pi}^{\pi} \mathbf{M}_f(e^{j\omega}) d\omega\end{aligned}$$

with

$$\begin{aligned}\mathbf{V}_f(z) &= \mathbf{L}_1(z) \mathbf{G}(z) \mathbf{W}(z) \mathbf{H}^*(z) \mathbf{S}^*(z) \mathcal{W}_M \mathbf{L}_2 \\ \mathbf{M}_f(z) &= \mathbf{M}_{f,1}(z) \odot \mathbf{M}_{f,2}^T(z) \\ &\text{and}\end{aligned}$$

$$\begin{aligned}\mathbf{M}_{f,1}(z) &= \mathbf{L}_2^* \mathcal{W}_M^* \mathbf{S}(z) \mathbf{H}(z) \mathbf{W}(z) \mathbf{H}^*(z) \mathbf{S}^*(z) \mathcal{W}_M \mathbf{L}_2 \\ \mathbf{M}_{f,2}(z) &= \mathbf{L}_1(z) \mathbf{L}_1^*(z).\end{aligned}$$

C. Optimization of $\mathbf{S}(z)$

In this section we assume that $h(z)$, $f(z)$, \mathbf{P} and \mathbf{Q} are fixed and we design $\mathbf{S}(z)$. Let $\underline{\mathbf{s}} = [\underline{\mathbf{s}}_1^T, \dots, \underline{\mathbf{s}}_{M^2}^T]^T$ be the column vector obtained by stacking up the samples of the impulse response $\mathbf{S}(t)$ of $\mathbf{S}(z)$, within the support defined by \mathbf{P} and \mathbf{Q} , i.e., for each $m, n = 1, \dots, M$,

$$\underline{\mathbf{s}}_{(n-1)M+m} = [[\mathbf{S}]_{m,n}(\mathbf{P}_{m,n}), \dots, [\mathbf{S}]_{m,n}(\mathbf{Q}_{m,n})]^T.$$

Also, define the following two transfer matrices

$$\begin{aligned}\mathbf{V}_S(z) &= \mathbf{F}(z) \mathbf{G}(z) \mathbf{W}(z) \mathbf{H}^*(z) \\ \mathbf{M}_S(z) &= \mathbf{H}(z) \mathbf{W}(z) \mathbf{H}^*(z) \otimes \mathbf{F}(z) \mathbf{F}^*(z)\end{aligned}$$

where $\mathbf{X}(z) \otimes \mathbf{Y}(z)$ denotes the Kronecker product, i.e., if $\mathbf{X}(z)$ and $\mathbf{Y}(z)$ have dimensions $B \times A$ and $D \times C$, respectively, $[\mathbf{X}(z) \otimes \mathbf{Y}(z)]_{bB+d, aA+c} = [\mathbf{X}(z)]_{b,a} [\mathbf{Y}(z)]_{d,c}$ for all a, b, c , and d . Then, we have

$$\underline{\mathbf{s}} = \underline{\mathbf{M}}_S^\dagger \mathbf{v}_S \quad (11)$$

where \mathbf{v}_S is obtained from $\mathbf{V}_S(z)$ in a way similar in which $\underline{\mathbf{s}}$ is obtained from $\mathbf{S}(z)$, after truncating the impulse response $\mathbf{V}_S(t)$ of $\mathbf{V}_S(z)$ so that its support is given by \mathbf{P} and \mathbf{Q} . Also, $\underline{\mathbf{M}}_S$ is the convolution matrix associated with $\mathbf{M}_S(z)$, i.e.

$$\underline{\mathbf{M}}_S = \begin{bmatrix} \underline{\mathbf{M}}_{S,1,1} & \cdots & \underline{\mathbf{M}}_{S,1,M^2} \\ \vdots & \ddots & \vdots \\ \underline{\mathbf{M}}_{S,M^2,1} & \cdots & \underline{\mathbf{M}}_{S,M^2,M^2} \end{bmatrix}$$

where for each $k, l, m, n = 1, \dots, M$

$$\begin{aligned}\underline{\mathbf{M}}_{S,i,j} &= \begin{bmatrix} \mathbf{M}_{S,i,j}(\mathbf{P}_{k,l} - \mathbf{Q}_{m,n}) & \cdots & [\mathbf{M}_S]_{i,j}(\mathbf{P}_{k,l} - \mathbf{P}_{m,n}) \\ \vdots & \ddots & \vdots \\ [\mathbf{M}_S]_{i,j}(\mathbf{Q}_{k,l} - \mathbf{Q}_{m,n}) & \cdots & [\mathbf{M}_S]_{i,j}(\mathbf{Q}_{k,l} - \mathbf{P}_{m,n}) \end{bmatrix} \\ &= \end{bmatrix}$$

with $i = (l-1)M + k$ and $j = (n-1)M + m$.

D. Choice of \mathbf{P} and \mathbf{Q}

Notice that the norm defined in (8) implicitly induces a Hilbert space of $D \times D$ transfer matrices with inner product

$$\langle \mathbf{X}, \mathbf{Y} \rangle_{\mathbf{W}} = \frac{1}{2\pi D} \int_{-\pi}^{\pi} \text{Tr} \{ \mathbf{X}(e^{j\omega}) \mathbf{W}(e^{j\omega}) \mathbf{Y}^*(e^{j\omega}) \} d\omega. \quad (12)$$

Consider the $M \times M$ impulses response matrices $\mathbf{U}_{m,n,\tau}(t)$, $m, n = 1, \dots, M$, $\tau \in \mathbb{Z}$ defined by

$$[\mathbf{U}_{m,n,\tau}(t)]_{i,j} = \begin{cases} 1, & i = m, j = n, t = \tau \\ 0 & \text{otherwise} \end{cases}$$

which form a basis for the space of all $M \times M$ transfer matrices. Then, we have that

$$\begin{aligned}\mathbf{V}_{m,n,\tau}(z) &= \mathbf{F}^*(z) \mathbf{U}_{m,n,\tau}(z) \mathbf{H}(z) \\ m, n &= 1, \dots, M, \tau \in \mathbb{Z}\end{aligned} \quad (13)$$

is a (possibly linearly dependent) set of $D \times D$ transfer matrices. Using this setting we can choose \mathbf{P} and \mathbf{Q} using any sparse approximation algorithm [24], [25] aiming at solving the following minimization problem:

$$[\mathbf{P}, \mathbf{Q}] = \arg \min_{\mathbf{P}, \mathbf{Q}: l_S} \arg \min_{\mathbf{S}: \mathbf{P}, \mathbf{Q}} \| \mathbf{G} - \mathbf{F}^* \mathbf{S} \mathbf{H} \|_{\mathbf{W}} \quad (14)$$

where the notation $\mathbf{P}, \mathbf{Q} : l_S$ means that the minimization over \mathbf{P} and \mathbf{Q} is constrained so that the total number of nonzero coefficients of the subband model $\mathbf{S}(z)$ equals l_S , and $\mathbf{S} : \mathbf{P}, \mathbf{Q}$ means that the minimization over \mathbf{S} is constrained so that its support is defined by \mathbf{P} and \mathbf{Q} . As aforementioned, we adapt the OMP algorithm [26], [27] to our problem, resulting in the

following iterative procedure. We begin by setting the estimate $\hat{\mathbf{G}}_0 = \mathbf{0}$, and at iteration k we compute

$$\begin{aligned} (m_k, n_k, \tau_k) &= \arg \max_{(m, n, \tau)} \frac{\left| \left\langle \mathbf{G} - \hat{\mathbf{G}}_{k-1}, \mathbf{V}_{m, n, \tau} \right\rangle_{\mathbf{W}} \right|}{\|\mathbf{V}_{m, n, \tau}\|_{\mathbf{W}}} \\ \hat{\mathbf{G}}_k &= \mathbf{F}^* \hat{\mathbf{S}}_k \mathbf{H} \\ \hat{\mathbf{S}}_k &= \arg \min_{\mathbf{S}: \mathbf{P}_k, \mathbf{Q}_k} \|\mathbf{G} - \mathbf{F}^* \mathbf{S} \mathbf{H}\|_{\mathbf{W}} \end{aligned} \quad (15)$$

where \mathbf{P}_k and \mathbf{Q}_k are defined so that they include all the indexes $\{(m_l, n_l, \tau_l) : l = 1, \dots, k\}$.

Remark 2: In order to simplify the computation of (15), we use (13) and Lemma 1 in the Appendix to get

$$\begin{aligned} &\left\langle \mathbf{G} - \hat{\mathbf{G}}_{k-1}, \mathbf{V}_{m, n, \tau} \right\rangle_{\mathbf{W}} \\ &= \left\langle \mathbf{F}(\mathbf{G} - \hat{\mathbf{G}}_{k-1}) \mathbf{W} \mathbf{H}^*, \mathbf{E}_{m, n, \tau} \right\rangle \\ &= \left[\mathcal{Z}^{-1} \left\{ \mathbf{F}(\mathbf{G} - \hat{\mathbf{G}}_{k-1}) \mathbf{W} \mathbf{H}^* \right\} \right]_{m, n}(\tau) \end{aligned}$$

where $\langle \cdot, \cdot \rangle$ denotes the inner product (12) with $\mathbf{W}(z) = 1$ for $|z| = 1$. All the inner products can be computed as the coefficients of the impulse response of the $M \times M$ transfer matrix $\mathbf{F}(z)(\mathbf{G}(z) - \hat{\mathbf{G}}_{k-1}(z))\mathbf{W}(z)\mathbf{H}^*(z)$. Also, notice that $\|\mathbf{V}_{m, n, \tau}\|_{\mathbf{W}}$ is independent of τ , i.e.

$$\|\mathbf{V}_{m, n, \tau}\|_{\mathbf{W}} = \|\mathbf{F}^* \mathbf{U}_{m, n, 0} \mathbf{H}\|_{\mathbf{W}}$$

for all $\tau \in \mathbb{Z}$, so only M^2 norms need to be computed at the beginning of the iteration process.

E. Initialization

The recursive method introduced above requires an initialization, since it is not guaranteed to converge to a global minimum of (7). To this end, we need to provide initial choices $h_0(z)$ and $f_0(z)$ for the filterbank prototypes $h(z)$ and $f(z)$, respectively. In the context of subband adaptive filtering, it was pointed out in [15] that a diagonal subband model leads to the most efficient subband configuration. In view of this, we propose to choose $h_0(z)$ and $f_0(z)$ so that the nonzero entries of the subband concentrate on the main diagonal as much as possible. To this end, we point out the following fact which follows from [14, Theorem 1]:

Lemma 1: If the frequency response of the analysis filters $h_m(z)$, $m = 1, \dots, M$ and the synthesis filters $f_m(z)$, $m = 1, \dots, M$ satisfy:

(C1) For each $m = 1, \dots, M$, the supports of $h_m(e^{j\omega})$ and $f_m(e^{j\omega})$ are contained in the same interval σ_m of measure $2\pi/D$,

(C2) The union $\cup_{m=1}^M \sigma_m$ of all M supports cover the whole interval $[-\pi, \pi]$, then, the approximation error can be made arbitrarily small using a diagonal subband model of sufficiently large tap size.

In view of Lemma 1, $h_0(z)$ and $f_0(z)$ need to minimize their stop-band energy. Hence, we design $h_0(z)$ as follows:

$$h_0(z) = \arg \min_{h_0(z): h_0(1)=1} \int_{\pi/D}^{2\pi-\pi/D} |h_0(e^{j\omega})|^2 d\omega$$

and we choose $f_0(z) = h_0(z)$.

V. OPTIMIZATION IN A LOGARITHMIC AMPLITUDE SCALE

As explained in Section I, in audio applications it is often more appropriate to replace the WLS criterion (1) by the following WLogLS criterion:

$$\begin{aligned} [h, f, \mathbf{S}] &= \arg \min_{h, f, \mathbf{S}, \mathbf{P}, \mathbf{Q}} \frac{1}{D} \sum_{d=0}^{D-1} \frac{1}{2\pi} \\ &\times \int_{-\pi}^{\pi} w(e^{j\omega}) \left| \log |g(e^{j\omega})| - \log |\hat{g}_d(e^{j\omega})| \right|^2 d\omega. \end{aligned} \quad (16)$$

A recursive algorithm for optimizing the parameters of a pole-zero transfer function in a WLogLS sense was proposed in [28]. Roughly speaking, that algorithm solves a weighted LLS problem whose weight is updated at each iteration. In this section we use this idea to modify the algorithm in Section IV to solve (16). The resulting algorithm is as follows:

- 1) **Initialization:** Obtain initial values of $h(z)$ and $f(z)$ as described in Section IV-E.
- 2) **Main iterations:** Cyclically iterate the following two steps, until the approximation error stops decreasing.
 - a) **WLS optimization:** Optimize $h(z)$, $f(z)$, $\mathbf{S}(z)$, \mathbf{P} , and \mathbf{Q} using the algorithm described in Section IV.
 - b) **Weight update:** Update the weight $\mathbf{W}(z)$ as described below.

As with the algorithm in [28], the proposed algorithm requires only a few (one or two) iterations to converge.

Let $\mathbf{C}(z)$ be the polyphase representation of $\log |g(z)|$ and $\hat{\mathbf{C}}(z)$ be that of $\log |\hat{g}_d(z)|$, $d = 0, \dots, D-1$. Then, we can write (16) as

$$[h, f, \mathbf{S}] = \arg \min_{h, f, \mathbf{S}, \mathbf{P}, \mathbf{Q}} \left\| \mathbf{C} - \hat{\mathbf{C}} \right\|_{\mathbf{W}}. \quad (17)$$

The idea is to iteratively solve (7), replacing at iteration k the weight $\mathbf{W}(z)$ by a weight $\mathbf{W}_k(z)$, so that the solution of (7) approximates that of (17).

Let $\mathbf{S}_k(z)$, $h_k(z)$ and $f_k(z)$ denote the values obtained at iteration k , and $\mathbf{H}_k(z)$ and $\mathbf{F}_k(z)$ denote the polyphase matrices of $h_k(z)$ and $f_k(z)$, respectively. Define $\hat{\mathbf{G}}_k(z) = \mathbf{F}_k^*(z) \mathbf{S}_k(z) \mathbf{H}_k(z)$ and $\tilde{\mathbf{G}}_k(z) = \mathbf{G}(z) - \hat{\mathbf{G}}_k(z)$. Also let $\hat{g}_{d,k}(z)$ denote the D -cyclostationary impulse responses obtained at iteration k , let $\hat{\mathbf{C}}_k(z)$ be the polyphase representation of $\log |\hat{g}_{d,k}(z)|$ and $\tilde{\mathbf{C}}_k(z) = \mathbf{C}(z) - \hat{\mathbf{C}}_k(z)$. We define the weight $\mathbf{W}_k(z)$ at iteration k by

$$\mathbf{W}_k(z) = \tilde{\mathbf{G}}_k^{-1}(z) \tilde{\mathbf{C}}_k(z) \mathbf{W}(z) \tilde{\mathbf{C}}_k^*(z) \tilde{\mathbf{G}}_k^{-*}(z). \quad (18)$$

Then, using (8), we have

$$\begin{aligned} [h_k, f_k, \mathbf{S}_k] &= \arg \min_{h, f, \mathbf{S}, \mathbf{P}, \mathbf{Q}} \|\mathbf{G} - \mathbf{F}^* \mathbf{S} \mathbf{H}\|_{\mathbf{W}_{k-1}} \\ &= \arg \min_{h, f, \mathbf{S}, \mathbf{P}, \mathbf{Q}} \left\| (\mathbf{G} - \mathbf{F}^* \mathbf{S} \mathbf{H}) \tilde{\mathbf{G}}_{k-1}^{-1} \tilde{\mathbf{C}}_{k-1} \right\|_{\mathbf{W}}. \end{aligned} \quad (19)$$

Hence, if the algorithm converges, we have that $\mathbf{G}(z) - \mathbf{F}_k^*(z) \mathbf{S}_k(z) \mathbf{H}_k(z) = \tilde{\mathbf{G}}_k(z) = \tilde{\mathbf{G}}_{k-1}(z)$ and therefore (20) is equivalent to (17).

VI. ILLUSTRATING EXAMPLES

In order to illustrate the applicability of the proposed method we consider two examples, one using the method described in

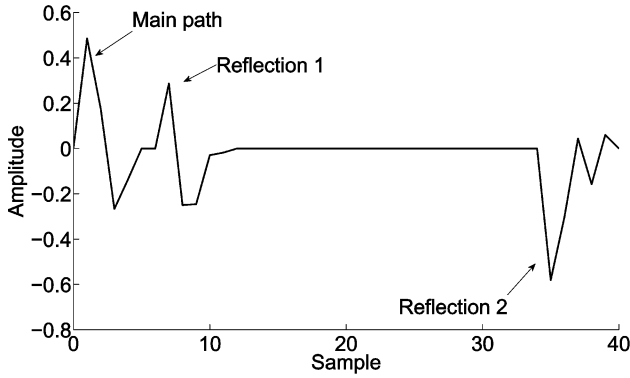


Fig. 3. Impulse response of the channel to be inverted.

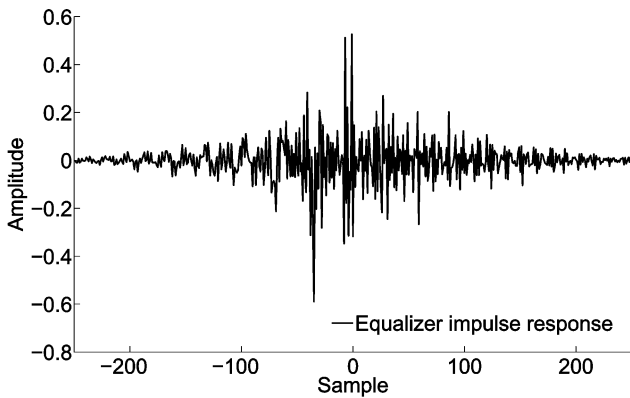


Fig. 4. Impulse response of the inverse channel.

Section IV for minimizing a WLS function, and the other using the method in Section V which minimizes a WLogLS function.

A. Example 1: Multipath Communication Channel Equalization

For the first example, we consider a channel equalization (i.e., inversion) problem for a communication channel whose impulse response is shown in Fig. 3, which resembles a multipath communication channel consisting of one main path and two reflections. The impulse response of the inverse channel is shown in Fig. 4.

We compare the performance obtained when approximating the inverse channel using segmented FFT (SFFT) methods, the zero-delay variant (ZD-SFFT) of the SFFT method which processes the first segment in the time domain, and the proposed subband method minimizing a WLS criterion (WLS-SB). The comparison is done in terms of computational cost, implementation latency, and approximation error. The latter is measured using the minimization argument in (1) with $w(e^{j\omega}) = 1$ for all $\omega \in [-\pi, \pi)$. Notice that $w(e^{j\omega}) = 1$ is the natural choice for the SFFT and ZD-SFFT methods, in which the inverse channel is approximated by truncating its impulse response.

For the SFFT and ZD-SFFT methods we truncate the equalizer impulse response so that its support is contained within the interval $[-223, 231]$, which achieves the minimum approximation error for a fixed impulse response length of 455 taps. By doing so we obtain an approximation error of -30.38 dB. For the WLS-SB method, we chose $M = 32$ subbands, a downsampling factor of $D = 20$, prototype tap sizes of $l_h = l_f = 100$

TABLE II
COMPARISON OF THE COMPUTATIONAL COST, LATENCY AND APPROXIMATION ERROR WHEN USING THE SFFT, THE ZD-SFFT AND THE WLS-SB METHOD

| | Comp. Cost | Latency | Rel. Err. |
|---------|---------------|--------------|-----------|
| SFFT | 59 mult./smp | 1593 samples | -30.38 dB |
| ZD-SFFT | 266 mult./smp | 223 samples | -30.38 dB |
| WLS-SB | 57 mult./smp | 199 samples | -30.71 dB |

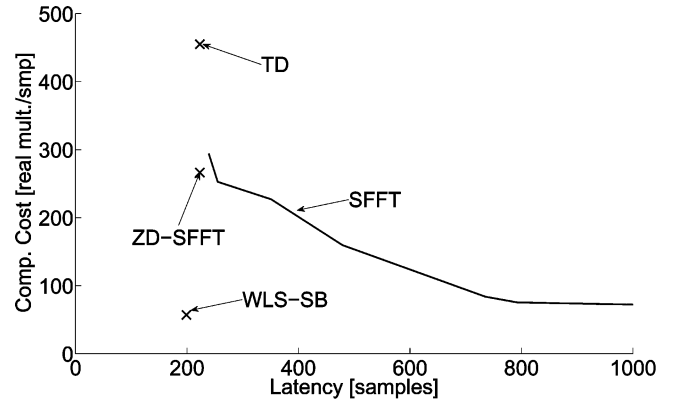


Fig. 5. Computation cost vs. latency of the different inverse channel implementation methods. All methods have similar approximation errors, as shown in Table II.

and we choose the total number of subband parameters l_S so that the maximum error is compatible with those of the SFFT and PZTF methods. To this end we choose $l_S = 320$ which produces an approximation error of -30.71 dB.

With the design above the SFFT, ZD-SFFT and WLS-SB methods have compatible approximation errors. So we compare in Fig. 7 their computational costs and latency values. In this comparison we also consider the time domain (TD) method, which directly implements the 455-tap truncated equalizer impulse response using direct convolution. The SFFT, ZD-SFFT and TD implementations have latency of 223, which is needed to make the equalizer impulse response causal. We observe that the ZD-SFFT method provides a significant improvement over the TD method in terms of computational cost, while keeping the same latency. The SFFT method is an attractive alternative only if large latency is allowed. On the other hand, the WLS-SB method offers an implementation slightly more efficient than the SFFT method, while introducing latency slightly smaller than those of the TD and ZD-SFFT methods.

We summarize the performance of the SFFT, ZD-SFFT, and WLS-SB methods in Table II. For the SFFT method we choose the configuration that most closely resembles the computational cost of the WLS-SB method. This is achieved when using one segment of 2048 samples. On the other hand, the ZD-SFFT method approximately matches the latency of the WLS-SB method. This is obtained using two segments of 128 samples, the first of which implemented in the time domain, followed by a third segment of 256 samples. We see that the WLS-SB method greatly outperforms the other two methods for the same latency or the same computational cost.

The comparison in Fig. 5 and Table II is for similar approximation errors for the TD, SFFT, ZD-SFFT, and WLS-SB methods. To see this, we show in Fig. 6 the frequency responses

of the models obtained using the four methods. Notice that the WLS-SB method is characterized not by one but by $D = 20$ frequency responses, since it is a D -cyclostationary system. However, all 20 systems are almost equivalent after optimizing the subband scheme using the proposed method.

B. Example 2: Implementation of Head-Related Transfer Functions

In the second example, we consider the implementation of HRTFs. We use a set of 1420 HRTFs (710 per ear), measured on a KEMAR dummy-head, publicly available from [29]. The HRTFs are 512 tap FIR filters (measured at 44.1 kHz) for the left and right ear. Following [30], we convert the HRTFs into minimum phase filters before processing.

We compare the performance obtained when implementing the HRTFs using the SFFT and ZD-SFFT methods, pole-zero transfer functions (PZTF) and the proposed subband method minimizing a WLogLS criterion (WLogLS-SB). Again, the comparison is done in terms of computational cost, latency and approximation error. For the latter, we use the following definition:

$$e_{\log} = \left(\frac{1}{b_{20k} - b_{20}} \int_{b_{20}}^{b_{20k}} \left| 20 \log_{10} \left| g(e^{j\omega(b)}) \right| - 20 \log_{10} \left| \hat{g}(e^{j\omega(b)}) \right|^2 db \right)^{1/2} \quad (21)$$

where b denotes the frequency in the Bark scale, i.e., if f denotes frequency in Hertz

$$b = 13 \times \arctan(0.00076 \times f) + 3.5 \times \arctan \left(\frac{f}{7500} \right)^2.$$

Also, $b_{20} = 0.1976$ and $b_{20k} = 24.58$ denote the Bark values of 20 Hz and 20 kHz, respectively, and $\omega(b)$ denotes the function which converts Barks to normalized angular frequency. Notice that for evaluating the error of the WLogLS-SB method, e_{\log} needs to be averaged over all $\hat{g}_d(z)$ as in (16). The error measure in (21) is similar to the one used in [31], except that we carry out the integration in the Bark frequency scale. To optimize e_{\log} using (16) we take $w(e^{j\omega}) = b'(\omega)$, where $b(\omega)$ denotes the function which converts normalized angular frequency to Barks, and $b'(\omega)$ denotes its derivative with respect to ω .

For the SFFT and ZD-SFFT methods, following [32], we truncate the HRTF's impulse responses to 5ms. (i.e., 221 taps). By doing so, the maximum approximation error over all available HRTFs is 2.644. For the PZTF method, we use the quasi-Newton algorithm in [9], initialized using the algorithm in [28], [31]. Following [9], we choose 40 poles and 40 zeros, which leads to a maximum error of 2.577. For the proposed WLogLS-SB method, as before, we chose $M = 32$ subbands, a downsampling factor of $D = 20$ and prototype tap sizes of $l_h = l_f = 100$, and we choose the total number of subband parameters l_S so that the maximum error is compatible with those of the SFFT, ZD-SFFT, and PZTF methods. This is met with $l_S = 192$ which leads to a maximum error of 2.537.

As before, the design above guarantees that the SFFT, ZD-SFFT, PZTF, and WLogLS-SB methods have compatible maximum approximation errors, and we compare in Fig. 7 their

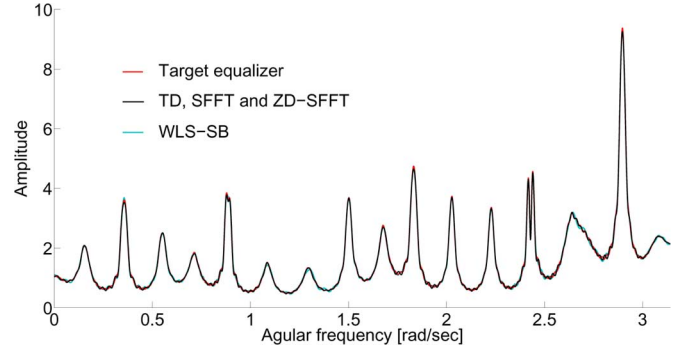


Fig. 6. Frequency response of the ideal inverse channel, and those of the implementations using the SFFT and the WLS-SB methods.

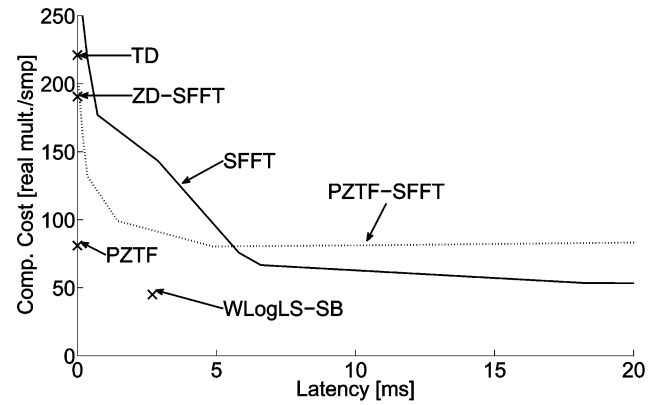


Fig. 7. Computation cost versus latency of the different HRTF implementation methods. All methods have similar approximation errors, as shown in Table III.

TABLE III
COMPARISON OF THE COMPUTATIONAL COST, LATENCY AND MAXIMUM APPROXIMATION ERROR WHEN USING THE SFFT, THE PZTF AND THE WLOGLS-SB METHOD

| | Comp. Cost | Latency | Max e_{\log} |
|-----------|---------------|----------|----------------|
| SFFT | 143 mult./smp | 2.9 ms. | 2.644 |
| SFFT | 52 mult./smp | 41.4 ms. | 2.644 |
| PZTF | 81 mult./smp | 0 ms. | 2.577 |
| WlogLS-SB | 45 mult./smp | 2.7 ms. | 2.537 |

computational costs and latencies. In this comparison we also consider the TD method and a hybrid PZTF-SFFT method in which the numerator is implemented using the SFFT method. In this case, the PZTF method provides an efficient implementation with zero latency. Only the SFFT and the WLogLS-SB methods are able to provide more efficient implementations than the PZTF method, but while doing so, the latency introduced by the WLogLS-SB method is clearly smaller than that of the SFFT method.

We summarize the performance of the SFFT, PZTF, and WLogLS-SB methods in Table III. For the SFFT method we consider two cases. In the first case, we aim at matching the latency of the WLogLS-SB method. We do so by using two segments of 256 samples. In the second case we aim at matching the computational cost of the WLogLS-SB method, for which we use one segment of 2048 samples. We see that the

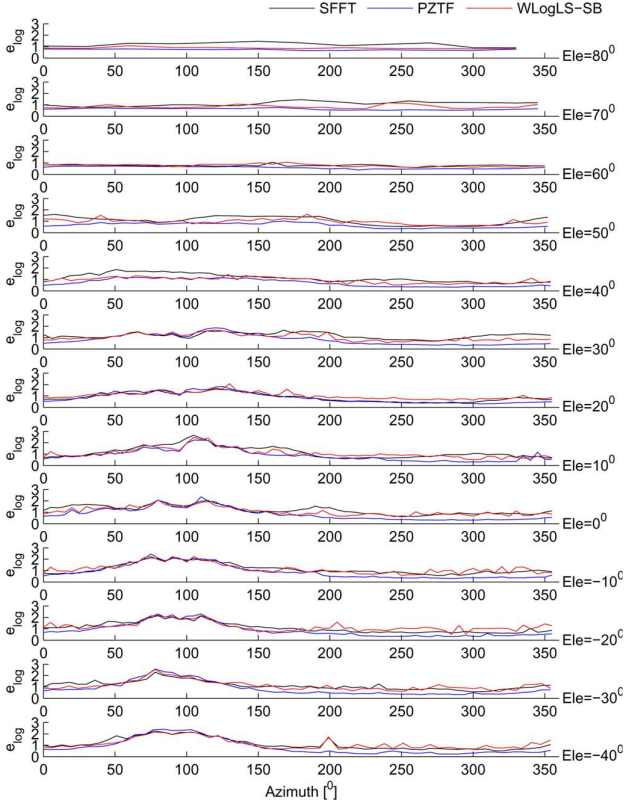


Fig. 8. Approximation errors obtained with the SFFT, the PZTF, and the WLogLS-SB method, when implementing all the HRTFs corresponding to the left ear. The approximation error is presented as a function of the azimuth and elevation (Ele).

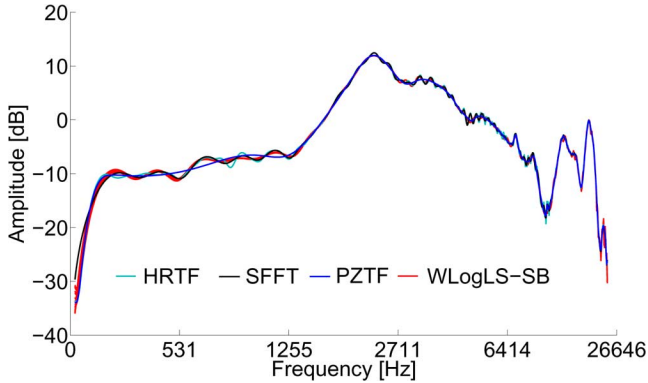


Fig. 9. Frequency response of the true HRTF (right ear, elevation = 0°, azimuth = 0°), the SFFT model ($\epsilon_{\log} = 0.95$), the PZTF model ($\epsilon_{\log} = 0.54$), and the WLogLS-SB model ($\epsilon_{\log} = 0.64$).

WLogLS-SB method largely outperforms the SFFT method for the same latency or the same computational cost, and that it is significantly more efficient than the PZTF method, although the latter introduces no latency.

Again, the comparison in Fig. 7 and Table II has similar maximum approximation errors for all the methods. We illustrate this by showing in Fig. 8 the approximation errors obtained using the SFFT, PZTF, and WLogLS-SB methods, for different azimuths and elevations. Also, in Fig. 9 we show the result obtained using the three methods for one particular direction.

VII. CONCLUSION

We have proposed an optimization method for approximating an LTI system using the subband technique. The proposed method optimizes the choices of subband model, analysis and synthesis filterbanks, including the optimal allocation of parameters from the different entries of the subband model. The proposed method has two versions. The first one carries out the optimization in a weighted least-squares sense in a linear amplitude scale, while the second one uses a logarithmic amplitude scale. We have presented results showing that, for a given approximation error, the proposed subband method can offer a more efficient implementation than the one obtained using a pole-zero transfer function and a better tradeoff between computational cost and latency than the one obtained using segmented FFT methods.

APPENDIX PROOFS

Proof of (7): Let $v(z)$ be such that $|v(e^{j\omega})|^2 = w(e^{j\omega})$ and define $\gamma(z) = g(z)v(z)$ and, for each $d = 1, \dots, D$, $\hat{\gamma}_d(z) = \hat{g}_d v(z)$. Then, (1) can be written as

$$\begin{aligned} [h, f, \mathbf{S}] &= \arg \min_{h, f, \mathbf{S}, \mathbf{P}, \mathbf{Q}} \frac{1}{D} \sum_{d=0}^{D-1} \frac{1}{2\pi} \\ &\quad \times \int_{-\pi}^{\pi} |\gamma(e^{j\omega}) - \hat{\gamma}_d(e^{j\omega})|^2 d\omega \\ &= \arg \min_{h, f, \mathbf{S}, \mathbf{P}, \mathbf{Q}} \frac{1}{D} \sum_{d=0}^{D-1} \sum_{t \in \mathbb{Z}} |\gamma(t) - \hat{\gamma}_d(t)|^2. \end{aligned}$$

Let $\mathbf{\Gamma}(z)$ and $\hat{\mathbf{\Gamma}}(z)$ be the polyphase representations of $\gamma(e^{j\omega})$ and $\hat{\gamma}_d(e^{j\omega})$, respectively, and define $\tilde{\mathbf{\Gamma}}(z) = \mathbf{\Gamma}(z) - \hat{\mathbf{\Gamma}}(z)$. Then, using (2) we obtain

$$\begin{aligned} [h, f, \mathbf{S}] &= \arg \min_{h, f, \mathbf{S}, \mathbf{P}, \mathbf{Q}} \frac{1}{D} \sum_{t \in \mathbb{Z}} \sum_{d, e=0}^{D-1} \left| [\tilde{\mathbf{\Gamma}}(t)]_{d, e} \right|^2 \\ &= \arg \min_{h, f, \mathbf{S}, \mathbf{P}, \mathbf{Q}} \frac{1}{2\pi D} \int_{-\pi}^{\pi} \sum_{d, e=0}^{D-1} \left| [\tilde{\mathbf{\Gamma}}(e^{j\omega})]_{d, e} \right|^2 d\omega \\ &= \arg \min_{h, f, \mathbf{S}, \mathbf{P}, \mathbf{Q}} \frac{1}{2\pi D} \int_{-\pi}^{\pi} \text{Tr} \left\{ \tilde{\mathbf{\Gamma}}(e^{j\omega}) \tilde{\mathbf{\Gamma}}^*(e^{j\omega}) \right\} d\omega. \end{aligned}$$

Now, $\hat{\gamma}_d(t)$, $d = 1, \dots, D$ is the impulse response obtained by the cascade of the LTI system with impulse response $v(t)$, followed by the D -cyclostationary system with impulse response $\hat{g}_d(t)$, $d = 1, \dots, D$. Hence, using (P2) in Section III-A, it follows that $\mathbf{\Gamma}(z) = \mathbf{G}(z)\mathbf{V}(z)$ and $\hat{\mathbf{\Gamma}}(z) = \mathbf{F}^*(z)\mathbf{S}(z)\mathbf{H}(z)\mathbf{V}(z)$, with $\mathbf{V}(z)$ being the polyphase representation of $v(z)$. Then, defining $\tilde{\mathbf{G}}(z) = \mathbf{G}(z) - \mathbf{F}^*(z)\mathbf{S}(z)\mathbf{H}(z)$ we have

$$\begin{aligned} [h, f, \mathbf{S}] &= \arg \min_{h, f, \mathbf{S}, \mathbf{P}, \mathbf{Q}} \frac{1}{2\pi D} \\ &\quad \times \int_{-\pi}^{\pi} \text{Tr} \left\{ \tilde{\mathbf{G}}(e^{j\omega}) \mathbf{V}(e^{j\omega}) \mathbf{V}^*(e^{j\omega}) \tilde{\mathbf{G}}^*(e^{j\omega}) \right\} d\omega \end{aligned}$$

$$\begin{aligned}
&= \arg \min_{h,f,\mathbf{S},\mathbf{P},\mathbf{Q}} \frac{1}{2\pi D} \\
&\quad \times \int_{-\pi}^{\pi} \text{Tr} \left\{ \tilde{\mathbf{G}}(e^{j\omega}) \mathbf{W}(e^{j\omega}) \tilde{\mathbf{G}}^*(e^{j\omega}) \right\} d\omega \\
&= \arg \min_{h,f,\mathbf{S},\mathbf{P},\mathbf{Q}} \left\| \tilde{\mathbf{G}} \right\|_{\mathbf{W}}
\end{aligned}$$

and the result follows. \blacksquare

Notation 1: The symbol $\mathcal{H}_{\mathbf{W}}^{A \times B}$ denotes the Hilbert space of $A \times B$ transfer matrices with inner product defined by (12), and $\mathcal{H}^{A \times B}$ refers to the case when $\mathbf{W}(z) = 1$ for $|z| = 1$.

Lemma 2: Consider the map $\Gamma : \mathcal{H}^{A \times B} \rightarrow \mathcal{H}_{\mathbf{W}}^{C \times D}$ defined by $\Gamma(\mathbf{X}) = \mathbf{U}\mathbf{X}\mathbf{V}$, then

$$\Gamma^*(\mathbf{Y}) = \mathbf{U}^* \mathbf{Y} \mathbf{W} \mathbf{V}^*.$$

Proof: We have that

$$\begin{aligned}
&\langle \mathbf{X}, \Gamma^*(\mathbf{Y}) \rangle \\
&= \langle \Gamma(\mathbf{X}), \mathbf{Y} \rangle_{\mathbf{W}} \\
&= \langle \mathbf{U}\mathbf{X}\mathbf{V}, \mathbf{Y} \rangle_{\mathbf{W}} \\
&= \frac{1}{2\pi D} \\
&\quad \times \int_{-\pi}^{\pi} \text{Tr} \{ \mathbf{U}(e^{j\omega}) \mathbf{X}(e^{j\omega}) \mathbf{V}(e^{j\omega}) \mathbf{W}(e^{j\omega}) \mathbf{Y}^*(e^{j\omega}) \} d\omega \\
&= \frac{1}{2\pi D} \\
&\quad \times \int_{-\pi}^{\pi} \text{Tr} \{ \mathbf{X}(e^{j\omega}) \mathbf{V}(e^{j\omega}) \mathbf{W}(e^{j\omega}) \mathbf{Y}^*(e^{j\omega}) \mathbf{U}(e^{j\omega}) \} d\omega \\
&= \langle \mathbf{X}, \mathbf{U}^* \mathbf{Y} \mathbf{W} \mathbf{V}^* \rangle
\end{aligned}$$

and the result follows since the equality holds for arbitrary \mathbf{X} and \mathbf{Y} . \blacksquare

Lemma 3: Let \mathcal{K} be a closed subspace of $\mathcal{H}^{A \times B}$ and $\Pi : \mathcal{H}^{A \times B} \rightarrow \mathcal{K}$ be the projection onto \mathcal{K} . Let Γ be the map defined in Lemma 1 and $\Gamma_{\mathcal{K}}$ be its restriction to \mathcal{K} . Then, the (Moore-Penrose) pseudoinverse [33] $\Gamma_{\mathcal{K}}^{\dagger}$ of $\Gamma_{\mathcal{K}}$ is given by

$$\Gamma_{\mathcal{K}}^{\dagger}(\mathbf{Y}) = \Upsilon^{\dagger} \Pi(\mathbf{U}^* \mathbf{Y} \mathbf{W} \mathbf{V}^*)$$

where the map $\Upsilon : \mathcal{K} \rightarrow \mathcal{K}$ is defined by

$$\Upsilon(\mathbf{X}) = \Pi(\mathbf{U}^* \mathbf{X} \mathbf{V} \mathbf{W} \mathbf{V}^*).$$

Proof: From a property of pseudoinverses, we have

$$\Gamma_{\mathcal{K}}^{\dagger} = (\Gamma_{\mathcal{K}}^* \Gamma_{\mathcal{K}})^{\dagger} \Gamma_{\mathcal{K}}^*. \quad (22)$$

Now, for all \mathbf{X} and \mathbf{Y} ,

$$\begin{aligned}
\langle \mathbf{X}, \Gamma_{\mathcal{K}}^*(\mathbf{Y}) \rangle &= \langle \Gamma_{\mathcal{K}}(\mathbf{X}), \mathbf{Y} \rangle_{\mathbf{W}} \\
&= \langle \Gamma(\mathbf{X}), \mathbf{Y} \rangle_{\mathbf{W}} \\
&= \langle \mathbf{X}, \Gamma^*(\mathbf{Y}) \rangle_{\mathbf{W}} \\
&= \langle \Pi \mathbf{X}, \Gamma^*(\mathbf{Y}) \rangle_{\mathbf{W}} \\
&= \langle \mathbf{X}, \Pi \Gamma^*(\mathbf{Y}) \rangle_{\mathbf{W}}
\end{aligned}$$

hence

$$\Gamma_{\mathcal{K}}^* = \Pi \Gamma^*. \quad (23)$$

and the result follows by putting (23) and Lemma 1 into (22). \blacksquare

Below, we use Lemma 3 to prove (9), (10), and (11).

Proof of (11): Let $\mathcal{K} \subset \mathcal{H}^{M \times M}$ be the subspace of sub-band models $\mathbf{S}(z)$ whose support is defined by the matrices \mathbf{N} and \mathbf{L} , and let $\Pi : \mathcal{H}^{A \times B} \rightarrow \mathcal{K}$ be the projection onto \mathcal{K} . Consider the map $\Gamma : \mathcal{H}^{M \times M} \rightarrow \mathcal{H}_{\mathbf{W}}^{D \times D}$ defined by $\Gamma(\mathbf{S}) = \mathbf{F}^* \mathbf{S} \mathbf{H}$. Then, the optimal subband model $\mathbf{S}(z)$ is given by

$$\mathbf{S} = \Gamma_{\mathcal{K}}^{\dagger}(\mathbf{G}).$$

Applying Lemma 3, we have

$$\mathbf{S} = \Upsilon^{\dagger} \Pi(\mathbf{F} \mathbf{G} \mathbf{W} \mathbf{H}^*)$$

with

$$\Upsilon(\mathbf{X}) = \Pi(\mathbf{F} \mathbf{F}^* \mathbf{X} \mathbf{H} \mathbf{W} \mathbf{H}^*).$$

Now, since \mathcal{K} is finite-dimensional (its dimension is l_S), the result follows by rearranging $\Pi(\mathbf{F} \mathbf{G} \mathbf{W} \mathbf{H}^*)$ into a column vector and the map $\mathbf{X} \mapsto \Pi(\mathbf{F} \mathbf{F}^* \mathbf{X} \mathbf{H} \mathbf{W} \mathbf{H}^*)$ into a matrix. \blacksquare

Proof of (9): Recall that l_h denotes the tap size of the analysis prototype $h(z)$, and let $\mathcal{K} \subset \mathcal{H}^{l_h \times l_h}$ be the subspace of $l_h \times l_h$ diagonal transfer matrices whose impulse response differs from zero only at $t = 0$, and let $\Pi : \mathcal{H}^{l_h \times l_h} \rightarrow \mathcal{K}$ be the projection onto \mathcal{K} . In this case, we use (4) to define the map $\Gamma : \mathcal{H}^{l_h \times l_h} \rightarrow \mathcal{H}_{\mathbf{W}}^{D \times D}$ by $\Gamma(\Lambda_h) = \mathbf{F}^* \mathbf{S} \mathcal{W}_M \mathbf{L}_2 \Lambda_h \mathbf{L}_1$, and following the steps above, the optimal matrix Λ_h is given by

$$\Lambda_h = \Upsilon^{\dagger} \Pi(\mathbf{L}_2^* \mathcal{W}_M^* \mathbf{S}^* \mathbf{F} \mathbf{G} \mathbf{W} \mathbf{L}_1^*)$$

with

$$\Upsilon(\mathbf{X}) = \Pi(\mathbf{L}_2^* \mathcal{W}_M^* \mathbf{S}^* \mathbf{F} \mathbf{F}^* \mathbf{S} \mathcal{W}_M \mathbf{L}_2 \mathbf{X} \mathbf{L}_1 \mathbf{W} \mathbf{L}_1^*)$$

and again, the result follows by arranging $\Pi(\mathbf{L}_2^* \mathcal{W}_M^* \mathbf{S}^* \mathbf{F} \mathbf{G} \mathbf{W} \mathbf{L}_1^*)$ into a column vector and $\mathbf{X} \mapsto \Pi(\mathbf{L}_2^* \mathcal{W}_M^* \mathbf{S}^* \mathbf{F} \mathbf{F}^* \mathbf{S} \mathcal{W}_M \mathbf{L}_2 \mathbf{X} \mathbf{L}_1 \mathbf{W} \mathbf{L}_1^*)$ into a matrix. \blacksquare

Proof of (10): This proof follows the steps of the proof above, taking into account the fact that the synthesis prototype $f(z)$ has real impulse response, which implies $\Lambda_f^* = \Lambda_f$. \blacksquare

REFERENCES

- [1] J. G. Proakis and D. G. Manolakis, *Digital Signal Processing: Principles, Algorithms, and Applications*, 3rd ed. Englewood Cliffs, NJ: Prentice-Hall Int., 1996.
- [2] W. Gardner, "Efficient convolution without input-output delay," *J. Audio Eng. Soc.*, vol. 43, no. 3, pp. 127–136, 1995.
- [3] M. Vorländer, *Auralization: Fundamentals of Acoustics, Modelling, Simulation, Algorithms and Acoustic Virtual Reality*, 1st ed. New York: Springer, 2008.
- [4] C. Sanathanan and J. Koerner, "Transfer function synthesis as a ratio of two complex polynomials," *IEEE Trans. Autom. Control*, vol. 8, pp. 56–58, 1963.
- [5] K. Steiglitz and L. McBride, "A technique for the identification of linear systems," *IEEE Trans. Autom. Control*, vol. AC-10, pp. 461–464, 1965.

- [6] A. Whitfield, "Asymptotic behaviour of transfer function synthesis methods," *Int. J. Contr.*, vol. 45, no. 3, pp. 1083–1092, 1987.
- [7] M. Blommer and G. Wakefield, "On the design of pole-zero approximations using a logarithmic error measure," *IEEE Trans. Signal Process.*, vol. 42, pp. 3245–3248, 1994.
- [8] J. Derby, "On the design of pole-zero approximations using a logarithmic error measure," *IEEE Trans. Signal Process.*, vol. 44, pp. 1811–1813, 1996.
- [9] M. Blommer and G. Wakefield, "Pole-zero approximations for head-related transfer functions using a logarithmic error criterion," *IEEE Trans. Speech Audio Process.*, vol. 5, pp. 278–87, 1997.
- [10] S. Gudvangen and S. Flockton, "Comparison of pole-zero and all-zero modelling of acoustic transfer functions (echo cancellation)," *Electron. Lett.*, vol. 28, no. 21, pp. 1976–1978, 1992.
- [11] S. Gudvangen and S. Flockton, "Modelling of acoustic transfer functions for echo cancellers," *Inst. Elect. Eng. Proc. Vision, Image Signal Process.*, vol. 142, no. 1, pp. 47–51, 1995.
- [12] P. Chanda and S. Park, "Immersive rendering of coded audio streams using reduced rank models of subband-domain head-related transfer functions," in *Proc. IEEE Int. Conf. Acoust., Speech Signal Process.*, 2006.
- [13] D. Marelli, "A functional analysis approach to subband system identification and approximation," *IEEE Trans. Signal Process.*, vol. 55, pp. 493–506, Feb. 2007.
- [14] D. M. Fu, "Performance analysis for subband identification," *IEEE Trans. Signal Process.*, vol. 51, pp. 3128–3142, Dec. 2003.
- [15] A. Gilloire and M. Vetterli, "Adaptive filtering in subbands with critical sampling: Analysis, experiments, and application to acoustic echo cancellation," *IEEE Trans. Signal Process.*, vol. 40, pp. 1862–1875, Aug. 1992.
- [16] Y. Lu and J. Morris, "Gabor expansion for adaptive echo cancellation," *IEEE Signal Process. Mag.*, vol. 16, no. 2, pp. 68–80, Mar. 1999.
- [17] D. Marelli and M. Fu, "A subband approach to channel estimation and equalization for dmt and ofdm systems," *IEEE Trans. Commun.*, vol. 53, pp. 1850–1858, Nov. 2005.
- [18] W. M. Hartmann, *Signals, Sound, and Sensation (Modern Acoustics and Signal Processing)*. New York: Amer. Inst. Phys., 2004.
- [19] F. Wightman and D. Kistler, "Headphone simulation of free-field listening. i. stimulus synthesis," *J. Acoust. Soc. Amer.*, vol. 85, no. 2, pp. 858–67, 1989.
- [20] F. Wightman and D. Kistler, "Headphone simulation of free-field listening. ii. psychophysical validation," *J. Acoust. Soc. Amer.*, vol. 85, no. 2, pp. 868–78, 1989.
- [21] S. Weiss and R. Stewart, "Fast implementation of oversampled modulated filter banks," *Electron. Lett.*, vol. 36, no. 17, pp. 1502–1503, Aug. 2000.
- [22] P. Vaidyanathan, *Multirate Systems and Filterbanks*. Englewood Cliffs, NJ: Prentice-Hall, 1993.
- [23] R. Fletcher, *Practical Methods of Optimization*, ser. A Wiley-Interscience Publication, 2nd ed. Chichester, U.K.: Wiley, 1987.
- [24] J. Tropp, "Greed is good: Algorithmic results for sparse approximation," *IEEE Trans. Inf. Theory*, vol. 50, pp. 2231–2242, 2004.
- [25] R. Baraniuk, "Compressive sensing," *IEEE Signal Process. Mag.*, vol. 24, no. 4, pp. 118–121, 2007.
- [26] G. Davis, S. Mallat, and Z. Zhang, "Adaptive time-frequency decompositions," *Opt. Eng.*, vol. 33, pp. 2183–2183, 1994.
- [27] Y. Pati, R. Rezaifar, and P. Krishnaprasad, "Orthogonal matching pursuit: Recursive function approximation with applications to wavelet decomposition," in *Conf. Rec. 27th Asilomar Conf. Signals, Syst. Comput.*, 1993, pp. 40–44.
- [28] T. Kobayashi and S. Imai, "Design of iir digital filters with arbitrary log magnitude function by wls techniques," *IEEE Trans. Acoust., Speech Signal Process.*, vol. 38, no. 2, pp. 247–52, 1990.
- [29] B. Gardner and K. Martin, Hrtf Measurement of a Kemar Dummy-Head Microphone 1994 [Online]. Available: <http://sound.media.mit.edu/KEMAR.html>
- [30] A. Kulkarni, S. Isabelle, and H. Colburn, "Sensitivity of human subjects to head-related transfer-function phase spectra," *J. Acoust. Soc. Amer.*, vol. 105, no. 5, pp. 2821–2840, 1999.
- [31] A. Kulkarni and H. Colburn, "Infinite-impulse-response models of the head-related transfer function," *J. Acoust. Soc. Amer.*, vol. 115, no. 4, pp. 1714–1728, 2004.
- [32] M. A. Senova, K. I. McAnally, and R. L. Martin, "Localization of virtual sound as a function of head-related impulse response duration," *J. Audio Eng. Soc.*, vol. 50, no. 1, pp. 57–66, Jan. 2002.
- [33] A. Ben-Israel and T. N. E. Greville, *Generalized Inverses*, ser. CMS Books in Mathematics/Ouvrages de Mathématiques de la SMC, 15, 2nd ed. New York: Springer-Verlag, 2003.



Damián Marelli received the Bachelors degree in electronics engineering from the Universidad Nacional de Rosario, Argentina, in 1995, the Ph.D. degree in electrical engineering and a Bachelor (Honors) degree in mathematics from the University of Newcastle, Australia, in 2003.

In 2003, he held a Research Associate position with the School of Electrical Engineering and Computer Science, University of Newcastle. In 2004 and 2005, he held a Postdoctoral Research Fellowship with the Laboratoire d'Analyse Topologie et Probabilités, CNRS/Université de Provence, France. Since 2006, he was a Research Academic with the ARC Centre for Complex Dynamic Systems and Control at the University of Newcastle. He held an Intra-European Marie Curie Fellowship with the Faculty of Mathematics, University of Vienna, Austria, from 2007 to 2008. His main research interests include multirate signal processing, time-frequency analysis, system identification, and statistical signal processing.



Minyue Fu (S'84–M'87–SM'94–F'04) received the Bachelor's degree in electrical engineering from the University of Science and Technology of China, Hefei, in 1982, and the M.S. and Ph.D. degrees in electrical engineering from the University of Wisconsin-Madison in 1983 and 1987, respectively.

From 1983 to 1987, he held a teaching assistantship and a research assistantship with the University of Wisconsin-Madison. He worked as a Computer Engineering Consultant with Nicolet Instruments, Inc., Madison, during 1987. From 1987 to 1989, he served as an Assistant Professor with the Department of Electrical and Computer Engineering, Wayne State University, Detroit, MI. For the summer 1989, he was with the Université Catholique de Louvain, Belgium, as a Maitre de Conférences Invited. He joined the Department of Electrical and Computer Engineering, University of Newcastle, Australia, in 1989. Currently, he is a Chair Professor in Electrical Engineering. In addition, he was a Visiting Associate Professor with the University of Iowa, Ames, during 1995–1996, and a Senior Fellow/Visiting Professor with Nanyang Technological University, Singapore (2002). He holds a ChangJiang Visiting Professorship with Shandong University and visiting positions with South China University of Technology and Zhejiang University in China. His main research interests include control systems, signal processing, and communications.

Dr. Fu has been an Associate Editor for the IEEE TRANSACTIONS ON AUTOMATIC CONTROL, *Automatica*, and the *Journal of Optimization and Engineering*.